Original article

Superior mediastinal cut-off measurements in chest radiographs for the screening of silent thoracic aortic diseases

Kantheera Leesmidt*, Boonyarit Sintuvikaiwong, Apichaya Sripariwuth

Department of Radiology, Faculty of Medicine, Naresuan University, Phitsanulok, Thailand

Abstract

Background: Analyzing the diagnostic cut-off values of chest radiographs provides an in-depth understanding of unrecognized aortic diseases, thereby contributing to a more comprehensive approach to identifying subtle aortic abnormalities.

Objectives: The objective of this study was to determine the cut-off measurements for superior mediastinal width and mediastinal width-to-thoracic cage ratio from chest radiographs for the early detection of unrecognized thoracic aortic diseases. In addition, this study aimed to enhance diagnostic strategies for identifying aortic abnormalities.

Methods: This retrospective analysis included 152 patients who underwent computed tomography angiography (CTA) of the thoracic aorta and chest radiograph between April 2007 and January 2021. Superior mediastinal width was measured at three levels on chest radiographs. Thoracic CTA findings were categorized into normal and abnormal groups, the latter comprising aortic dissection, intramural hematoma, penetrating atherosclerotic ulcer, and aneurysm. The cut-off values for the superior mediastinal width and mediastinal width-to-thoracic cage ratio were calculated using receiver operating characteristic (ROC) curve analysis.

Results: The optimal cut-off values were a mediastinal width ≥ 8.4 cm at the aortic knob level (ROC 77.3, 95% confidence interval (CI) 69.8–84.9, $P < 0.001$; sensitivity 72.7%, specificity 71.1%, positive predictive value (PPV) 58.8%, negative predictive value (NPV) 82.1%) and a mediastinal width-to-thoracic cage ratio ≥ 0.294 at the same level (ROC 78.6, 95% CI 70.8–86.3, $P < 0.001$; sensitivity 80.0%, specificity 61.9%, PPV 54.3%, NPV 84.5%).

Conclusion: The established superior mediastinal width and ratio cut-off values from chest radiographs can aid clinicians in identifying patients who are at risk for silent thoracic aortic disease, prompting further CTA evaluation that can prevent fatal outcomes and improve patients' quality of life.

Keywords: Chest radiograph, cut-off values, mediastinal measurement, nontraumatic aortic disease, widening of mediastinum.

The early diagnosis of aortic rupture remains a challenge, particularly in patients with underlying cardiovascular diseases who present with asymptomatic or nonspecific clinical features.[1–6] Aortic rupture is a life-threatening complication that is associated with high morbidity and mortality rates.[7–12] While numerous studies have demonstrated the diagnostic accuracy of computed tomography (CT) in evaluating aortic pathology,[1, 13–23] routine screening with CT remains limited because of radiation exposure and the risk of developing contrast-induced nephropathy, especially in patients with compromised renal function.[24–31]

Conversely, chest radiography is a widely available, cost-effective, and noninvasive imaging technique that entails minimal radiation exposure and does not necessitate contrast agents.[32] It is a valuable initial screening tool and diagnostic modality for various pulmonary and cardiac diseases, particularly in emergency department settings.[33] Notably, the

***Correspondence to: Kantheera Leesmidt**, Department of Radiology, Faculty of Medicine, Naresuan University, Phitsanulok 65000, Thailand.
E-mail: kantheeral@nu.ac.th
Received: August 9, 2025
Revised: January 22, 2026
Accepted: February 4, 2026

Open Access 2026 Leesmidt., published by Faculty of Medicine, Chulalongkorn University. This work is licensed under the Creative Commons Attribution 4.0 International License.

aortic silhouette can often be visualized on chest radiographs, and therefore, the recognition of abnormal findings on these chest radiographs may facilitate the early detection of aortic disease and help prevent life-threatening consequences.

This study aimed to establish diagnostic cut-off values for the superior mediastinal width and width-to-thoracic cage ratio on chest radiographs to aid in the identification of silent thoracic aortic disease. This approach may assist clinicians in recognizing patients who are at-risk, particularly those without trauma or suspicious symptoms, and may benefit from further evaluation with computed tomography angiography (CTA).

Materials and methods

This retrospective study was reviewed and approved by the Naresuan University Institutional Review Board (IRB protocol no. P3-0020/2563), and imaging findings were correlated with clinical parameters.

The study analyzed chest radiographs to determine the superior mediastinal measurements for detecting asymptomatic or subclinical aortic diseases in patients without traumatic injuries. A total of 452 patients who underwent CTA of the thoracic aorta between April 2007 and January 2021 were initially reviewed. Of these, 64 pediatric patients under 15 years of age were excluded. Furthermore, patients whose chest radiographs showed evidence of aortic surgical materials or were not obtained within one month of the CTA were excluded. A review of clinical data from the medical records revealed that none of the patients exhibited chest pain or other typical symptoms that were suggestive of thoracic aortic disease. After applying these criteria, 152 patients were included in the final analysis. **Figure 1** shows the flow of patients through the study.

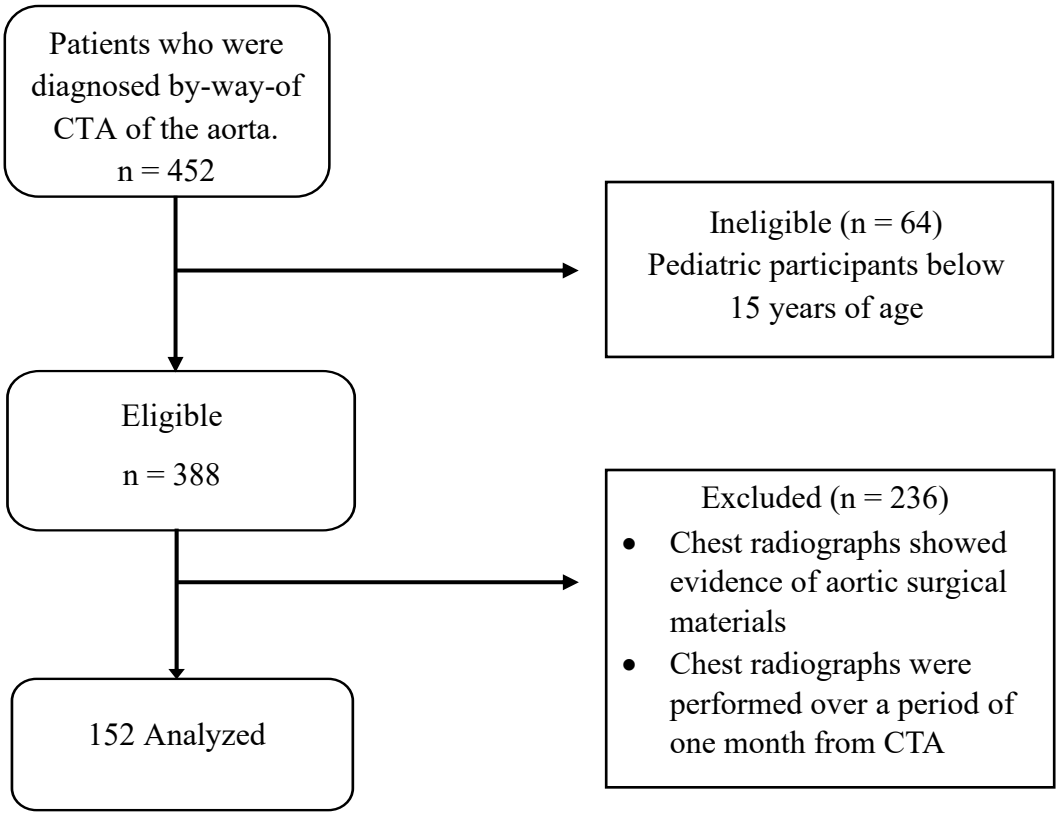

Figure 1. Flow chart represents the selection of the study population. CTA, computed tomography angiography.

Demographic data, including sex, age, weight, and height, were recorded, and body surface area (BSA) was calculated using the Mosteller formula. These parameters were analyzed to assess the influence of body size and to validate the generalizability of the proposed cut-off values. Chest radiography was performed using the posteroanterior (PA) projection with patients in the upright position. All patients were instructed to maintain full inspiration during image acquisition. The source-to-image distance was standardized at 180 cm.

To ensure accuracy of the measurement, two investigators (KL and AS) were blinded to the CTA findings and independently reviewed the chest radiographs. The superior mediastinal width was measured at three anatomical levels, namely 1) the aortic knob; 2) the carina; and 3) the widest portion of the superior mediastinum **(Figure 2)**. The measurement was defined as the maximum horizontal distance between the right and left lateral borders of the superior mediastinal shadow.

The CTA images and initial chest radiographs were reviewed and assessed at separate times to minimize interpretation bias. The CTA findings were categorized into normal and abnormal groups. Aortic diseases classified in the abnormal group included aortic dissection **(Figure 3A)**, intramural hematoma (IMH) **(Figure 3A)**, saccular aneurysm **(Figure 3B)**, penetrating atherosclerotic ulcer (PAU) **(Figure 3C)**, and fusiform aneurysm **(Figure 3D)**. According to current medical guidelines, a fusiform thoracic aortic diameter ≥ 5.5 cm is considered aneurysmal and places patients at increased risk of serious complications, which often require surgical intervention even in the absence of known aortic disease. [34, 35] In this study, this threshold was used for aortic aneurysm identification. Aortic diameters were measured at four anatomical levels, namely the midascending aorta, distal ascending aorta, aortic arch, and middescending aorta, using axial cross-sections perpendicular to the direction of blood flow with multidimensional reconstructions **(Figure 4)**.

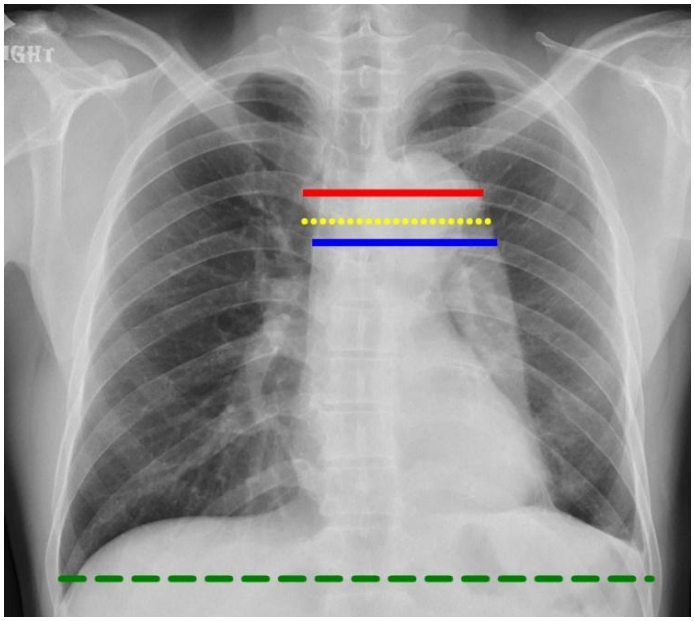

Figure 2. Superior mediastinal and thoracic cage measurements on chest radiograph. Schematic illustration showing the method for measuring superior mediastinal width at 3 levels: the aortic knob (red solid line), the widest superior mediastinum (yellow dotted line), and the carina (blue solid line). The superior mediastinal width at each level was determined by the longest horizontal distance between the right and left lateral borders of the superior mediastinal shadow. Specifically, the aortic knob level measurement extends from the right lateral border of the superior mediastinum to the left lateral border of the aortic knob. The widest superior mediastinum represents the maximal horizontal measurement between the right and left mediastinal interfaces. The carina level measurement is taken at the point of tracheal bifurcation, applying the same method. The thoracic cage width (green dashed line) is measured as the longest horizontal distance between the inner borders of the ribs on both sides at the level of the diaphragm.

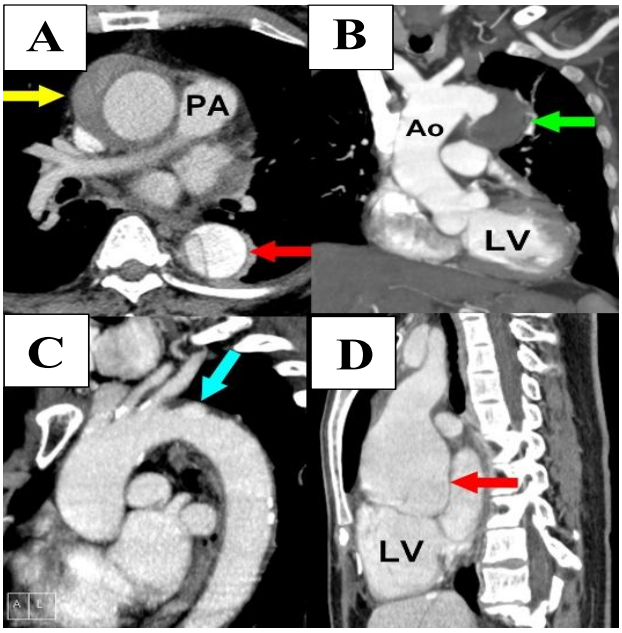

Figure 3. Examples of CTA demonstrating with aortic pathology. **(A)** axial CT image at the main pulmonary artery level showing a crescent-shaped, non-enhancing IMH at the ascending aorta (yellow arrow) and a double aortic lumen with an intimal flap indicative of aortic dissection at the descending aorta (red arrow), **(B)** coronal oblique CTA view illustrating an out-pouching lesion of a partially thrombosed saccular aneurysm arising from the proximal descending aorta (green arrow), **(C)** sagittal oblique view ("candy cane" view) CTA view revealing a non-calcified atheromatous plaque with a PAU at the proximal descending aorta (blue arrow), located just distal to the origin of the left subclavian artery, **(D)** sagittal CT image showing a fusiform aneurysm of the aortic root (red arrow). Ao, aorta; CT, computed tomography; CTA, computed tomography angiography; IMH, intramural hematoma; LV, left ventricle; PA, pulmonary artery; PAU, penetrating atherosclerotic ulcer.

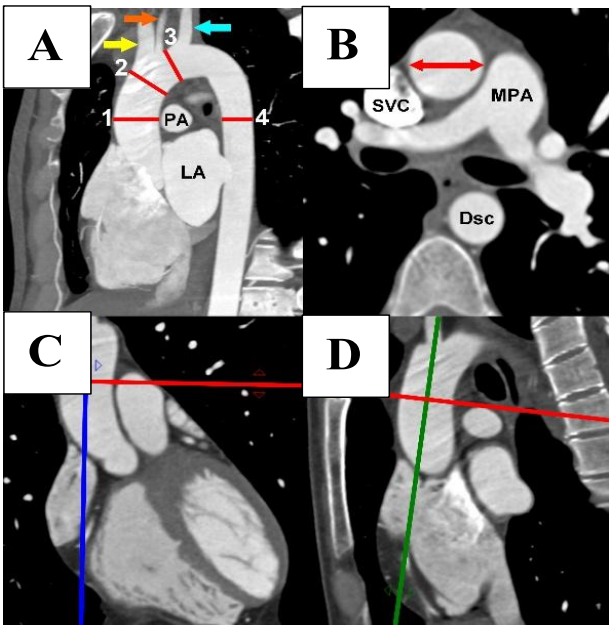

Figure 4. Example of CTA with aortic diameter measurements. **(A)** sagittal oblique view ("candy cane" view) of the thoracic aorta showing four designated measurement points: 1) mid-ascending aorta at the level of the pulmonary artery; 2) distal ascending aorta, slightly proximal to the origin of the innominate artery (yellow arrow); 3) aortic arch, between the origins of the left common carotid artery (orange arrow) and the left subclavian artery (light blue arrow); and 4) mid-descending aorta at the level of the pulmonary artery, **(B)** axial CT image illustrating the measurement of the ascending thoracic aorta along an axis perpendicular to the direction of blood flow (red double-headed arrow), **(C, D)** coronal and sagittal CT images demonstrating the application of multidimensional reconstructions, confirming that all measurements are accurately aligned perpendicular to the direction of blood flow. CT, computed tomography; Dsc, descending thoracic aorta; LA, left atrium; MPA, main pulmonary artery; PA, pulmonary artery; SVC, superior vena cava.

Statistical analysis

Data were expressed as the mean ± standard deviation (SD). Receiver operating characteristic curve (ROC) analysis was used to determine the optimal cut-off values for the mediastinal width and mediastinal width-to-thoracic cage ratio for predicting thoracic aortic disease. Sensitivity, specificity, and positive and negative predictive values (PPV and NPV, respectively) were calculated. A two-tailed $P < 0.05$ was considered statistically significant. Correlations between the mediastinal and thoracic cage widths, as well as between the mediastinal width and BSA, were evaluated using Pearson's correlation test. Statistical analysis was performed using Stata version 12.0 (StataCorp, College Station, TX, USA).

Results

The median age of patients was 65 years (range: 26–93 years). The cohort consisted of 100 males (65.8%) and 52 females (34.2%). The data on gender, age, weight, height, and BSA of all patients are shown in **Table 1.**

The superior mediastinal measurements at all levels on chest radiographs are summarized in **Table 2.** Thoracic aortic disease was identified on CTA in 55 patients (36.2%, 95% confidence interval (CI) 28.6–44.4). Combined aortic pathologies were observed in seven patients, including aneurysm with dissection (n = 3), aneurysm with PAU (n = 1), IMH with dissection (n = 1), IMH with concealed aneurysmal rupture (n = 1), and concurrent fusiform aneurysm of the ascending aorta with saccular aneurysm involving the aortic arch and proximal descending aorta (n = 1). The remaining 97 patients (63.8%) had normal CTA findings.

The correlation among the aortic measurements, thoracic cage, and BSA was performed using Pearson's correlation coefficient, as shown in **Table 3.** Diagnostic performance metrics, including sensitivity, specificity, PPV, NPV, and area under the ROC curve (AUC), are presented in **Table 4.**

Table 1. Subject's characteristic data (n = 152).

Characteristic data	n = 152
Gender; n (%)	
Male	100 (65.8%)
Female	52 (34.2%)
Age (years) (mean ± SD)	64.6 ± 15.4
Weight (kg) (mean ± SD)	60.6 ± 13.2
Height (cm) (mean ± SD)	161.8 ± 9.9
BSA (m^2) (mean ± SD)	1.6 ± 0.2

BSA, body surface area; SD, standard deviation.

Table 2. Superior mediastinal width measurements and mediastinal width-to-thoracic cage ratios on chest radiographs (n = 152).

Measurements	Mean ± SD (cm or ratio)
Aortic knob (cm)	8.5 ± 1.7
Carina (cm)	9.2 ± 1.9
Widest superior mediastinum (cm)	9.7 ± 2.0
Thoracic cage (cm)	28.2 ± 2.6
Aortic knob / thoracic cage ratio	0.3 ± 0.1
Carina / thoracic cage ratio	0.3 ± 0.1
Widest superior mediastinum / thoracic cage ratio	0.4 ± 0.1

* Values are presented as mean ± SD

Table 3. Correlation between aortic diameters, thoracic cage, and BSA.

	Aortic diameters					
Factor	**Aortic knob**		**Carina**		**Superior mediastinum**	
	r	***P*-value**	***r***	***P*-value**	***r***	***P*-value**
Thoracic cage	0.133	0.103	0.045	0.581	0.057	0.486
BSA	0.138	0.090	0.154	0.058	0.130	0.111

BSA, body surface area.

Table 4. Diagnostic performance of mediastinal width and mediastinal width-to-thoracic cage ratio for screening thoracic aortic pathology (n = 152).

Measurement	AUC (%) (95%CI)	Sensitivity (%) (95%CI)	Specificity (%) (95%CI)	PPV (%) (95%CI)	NPV (%) (95%CI)	*P*-value
Aortic knob ≥ 8.4 cm	77.3 (69.8–84.9)	72.7 (65.7–79.8)	71.1 (63.9–78.3)	58.8 (51.0–66.7)	82.1 (76.1–88.2)	< 0.001
Carina ≥ 8.7 cm	76.4 (68.9–83.8)	76.4 (69.6–83.1)	62.9 (55.2–70.6)	53.9 (45.9–61.8)	82.4 (76.4–88.5)	< 0.001
Widest superior mediastinum ≥ 9.8 cm	74.2 (66.4–82.0)	70.9 (63.7–78.1)	68.0 (60.6–75.4)	55.7 (47.8–63.6)	80.5 (74.2–86.8)	< 0.001
Aortic knob / Thoracic cage ≥ 0.294	78.6 (70.8–86.3)	80.0 (73.6–86.4)	61.9 (54.1–69.6)	54.3 (46.4–62.2)	84.5 (78.8–90.3)	< 0.001
Carina / Thoracic cage ≥ 0.326	76.8 (69.3–84.2)	72.7 (65.6–79.8)	70.1 (62.8–77.4)	58.0 (50.1–65.8)	81.9 (75.8–88.0)	< 0.001
Widest superior mediastinum / Thoracic cage ≥ 0.330	74.7 (66.8–82.6)	78.2 (71.6–84.7)	60.8 (53.1–68.6)	53.1 (45.2–61.0)	83.1 (77.1–89.1)	< 0.001

AUC values 0.7 and 0.8 indicate considered acceptable discrimination. AUC, area under the ROC curve, NPV, negative predictive value; PPV, positive predictive value; ROC, receiver operating characteristic.

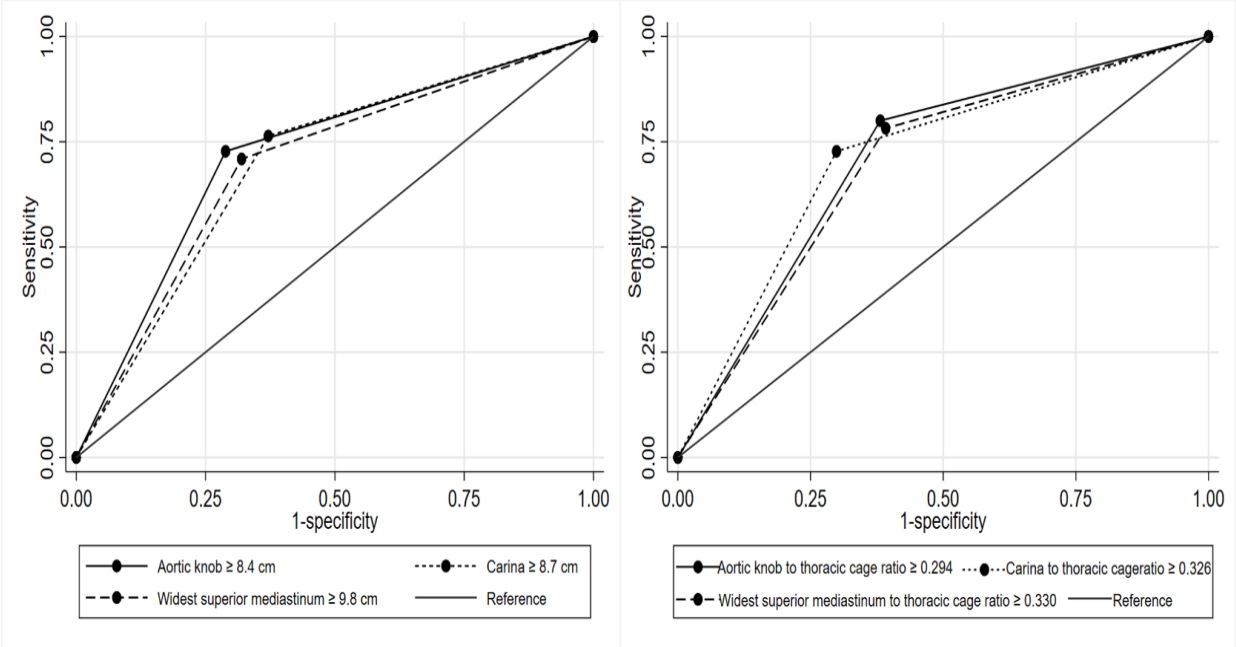

Figure 5. Area under ROC curves for mediastinal width and mediastinal width-to-thoracic cage ratio at the aortic knob level. The optimal cut-off points were ≥ 8.4 cm for mediastinal width (AUC 77.3, $P < 0.001$) and ≥ 0.294 for the ratio (AUC 78.6, $P < 0.001$), demonstrating acceptable diagnostic performance for detecting thoracic aortic pathology. AUC, area under the ROC curve; ROC, receiver operating characteristic.

The highest AUC values were observed at the aortic knob level, with an optimal cut-off point of ≥ 8.4 cm for the mediastinal width. This yielded an AUC of 77.3% (95% CI 69.8–84.9, $P < 0.001$) with a sensitivity of 72.7%, specificity of 71.1%, PPV of 58.8%, and NPV of 82.1%. For the mediastinal width-to-thoracic cage ratio, a cut-off point of ≥ 0.294 produced an AUC of 78.6% (95% CI 70.8–86.3, $P < 0.001$), with a sensitivity of 80.0%, specificity of 61.9%, PPV of 54.3%, and NPV of 84.5%. These thresholds demonstrated the most effective parameters identified in our evaluation of the superior mediastinal width **(Figure 5)**. No significant correlation was observed between the superior mediastinal and thoracic cage widths, nor between the superior mediastinal width and BSA ($P > 0.05$).

Discussion

An overview of the study workflow and the principal findings are presented in **Figure 6**. This study revealed that the NPVs of the proposed cut-off points for the mediastinal width and mediastinal width-to-thoracic cage ratio in chest radiographs offer valuable insight into identifying silent aortic diseases in asymptomatic individuals. All identified cut-off values yielded significant results with NPVs exceeding 80.0% within the 95% CI. Furthermore, the absence of a significant correlation between the superior mediastinal width and BSA suggests that these numbers of measurements and ratios can be broadly applied for the screening of aortic diseases in patients regardless of variations in body size.

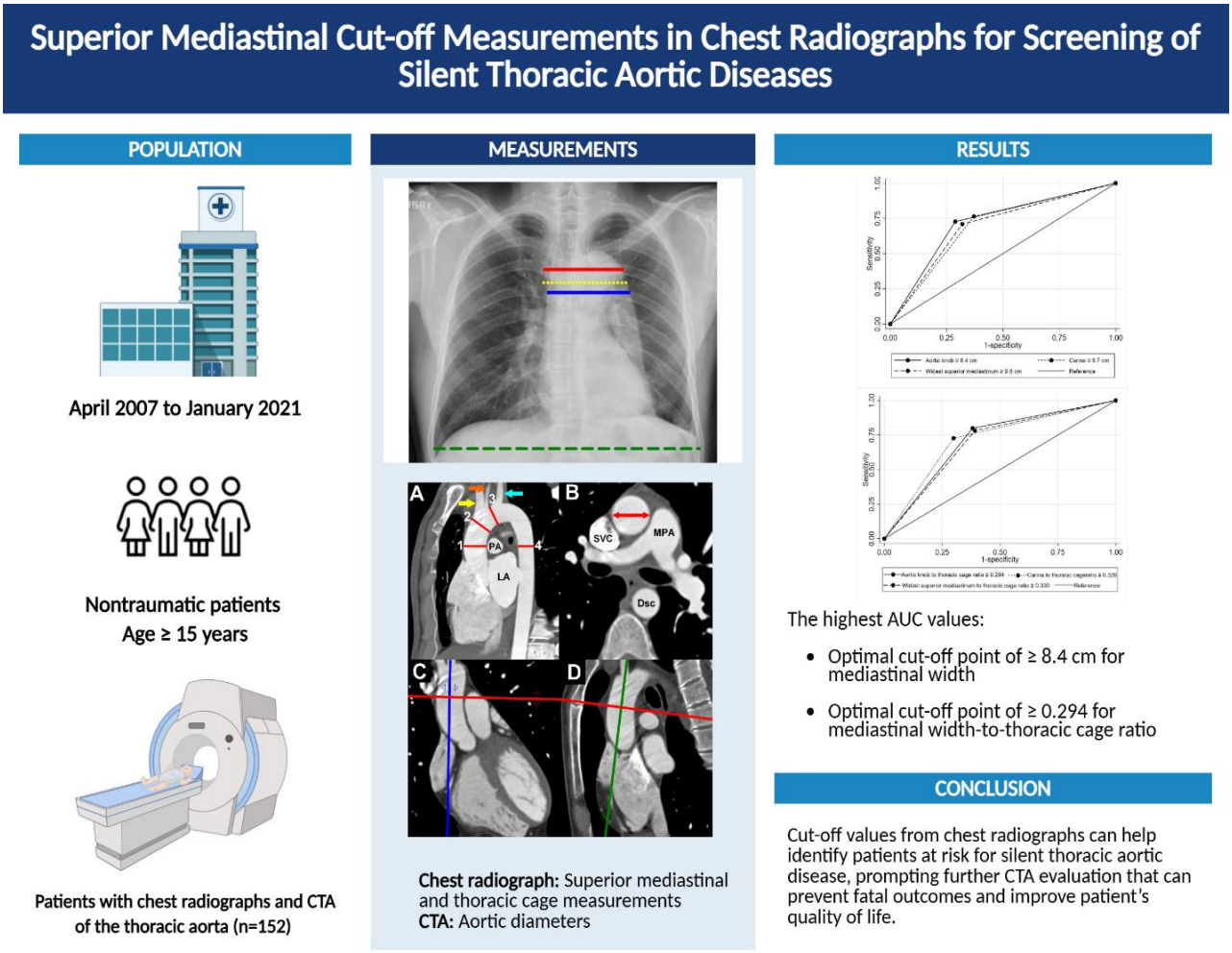

Figure 6. An overview of the study workflow and principal findings. AUC, area under curve; CTA, computed tomography angiography; DSC, descending thoracic aorta; LA, left atrium; MPA, main pulmonary artery; PA, pulmonary artery; SVC, superior vena cava.

Among the evaluated parameters, a mediastinal width ≥ 8.4 cm and a mediastinal width-to-thoracic cage ratio > 0.294 at the aortic knob level exhibited the strongest diagnostic performance for identifying nontraumatic aortic abnormalities. These findings are consistent with previous studies,[36–38] such as those by Fultz PJ and Seltzer SE, which reported comparable thresholds. Fultz PJ, *et al*. evaluated the features of chest radiographs in patients with nontraumatic mediastinal hemorrhage following thoracic aortic aneurysm rupture, dissection, or penetrating ulcers.[36] They also found that a superior mediastinal width ≥ 8 cm and a mediastinal width-to-chest width ratio > 0.25 on supine radiographs, with obscuration or bulging of the aortopulmonary window and a shifted left paraspinal line, were indicative of mediastinal hemorrhage.[36]

Similarly, Seltzer SE, *et al*. investigated the mediastinal width-to-chest width ratios in patients with blunt chest trauma to refine diagnostic approaches.[37] Their study evaluated the significance at three anatomical levels (aortic arch, midascending aorta, and middescending aorta) and suggested that an aortic level ratio > 0.25 could indicate an aortic rupture, thus potentially making further invasive procedures for those without rupture unnecessary.[37]

It should be noted; however, that these cut-off values may have limited sensitivity in patients with aortic-related connective tissue disorders; therefore, these populations fall outside the scope of this study. In those cases, more sensitive imaging modalities or tailored criteria may be necessary. In addition, the threshold of an aortic diameter ≥ 5.5 cm remains a widely accepted indicator for the diagnosis of an aortic aneurysm and determining the need for surgical intervention.

Underlying conditions that may influence aortic measurements, including connective tissue disorders, aortic valve pathology, and long-standing hypertension, were not evaluated as study variables. However, patients with visible surgical materials on chest radiograph images were excluded, as these findings were presumed to indicate previous aorta-related surgical intervention.

This study has some limitations. Pham MHC, *et al*. reported that the overall prevalence of aortic aneurysms in the total population was 2.1%.[39] Notably, 36.0% of the included patients in our study had confirmed aortic pathology, thus indicating that the derived cut-off values were based on a cohort with a relatively high proportion of abnormal findings. The findings of this study are more reflective of risk thresholds than normative values intended for general population-based screening. Future research with larger sample sizes and a broader demographic representation is required to establish more generalizable reference values. Moreover, chest radiographic technique may influence the study results. The cut-off values in this study were derived from radiographs obtained using PA projection with patients in an upright position and a standardized source-to-image distance of 180 cm. Differences in patient positioning or imaging distance may influence the mediastinal measurements and could potentially affect the sensitivity and specificity of the proposed cut-off values. Interobserver variability between the two readers was qualitatively assessed without further statistical analysis. Additional studies incorporating formal interobserver agreement statistics would be valuable to validate the sensitivity, specificity, PPV, and NPV of these cut-off values.

Furthermore, relying solely on a mediastinal width of 8.4 cm and a width-to-thoracic cage ratio of 0.294 at the aortic knob level may overlook the presence of other aortic diseases. Although our findings suggest that aortic pathology often originates from a single location within the superior mediastinum, some cases involved a combination of aortic abnormalities at multiple levels. Therefore, evaluating the superior mediastinal measurements at all assessed levels using the cut-off values may provide a more comprehensive screening approach for the detection of asymptomatic or nonspecific thoracic aortic disease.

Conclusion

The findings of this study highlight the importance of effective diagnostic tools in the management of aortic disease. The six cut-off values for the mediastinal width derived from chest radiographs present a valuable screening approach for the detection of occult, nontraumatic thoracic aortic conditions. Their application can assist clinicians in triaging patients for further CTA evaluation, which is essential for preventing fatal outcomes and improving patient prognosis. Moreover, this approach promotes a balanced perspective on diagnostic strategies, weighing the benefits of early detection against concerns related to radiation exposure and contrast agent use.

Author contributions

KL and AS contributed substantially to the concept and design of this study, acquiring the data, reviewing literature, and its analysis and interpretation. BS contributed substantially to acquiring the data. KL contributed to drafting the manuscript. KL and AS edited the manuscript critically for important intellectual content. All authors approved the final version submitted for publication and take responsibility for statements made in the published article.

Acknowledgments

The authors would like to extend their gratitude to the International Relations Section of the Faculty of Medicine, Naresuan University, for English language editing assistance and to Miss Kornthip Jeephet of the Clinical Epidemiology and Clinical Statistics Unit, Faculty of Medicine, Naresuan University, for her assistance in statistical analysis.

Conflicts of interest statement

The authors have each completed the International Committee of Medical Journal Editors Form for uniform Disclosure of Potential Conflicts of Interest. No authors have any potential conflict of interest to disclose/None of the authors disclose any potential conflict of interest.

Data sharing statement

All data generated or analyzed in the present study are included in the published article. Further details are available for non-commercial purposes from the corresponding author upon reasonable request.

ORCID

Kantheera Leesmidt : https://orcid.org/0000-0003-2563-1557
Boonyarit Sintuvikaiwong: https://orcid.org/0009-0007-5453-9035
Apichaya Sripariwuth : https://orcid.org/0000-0001-7735-5887

References

1. Holloway BJ, Rosewarne D, Jones RG. Imaging of thoracic aortic disease. Br J Radiol. 2011;84 Spec No 3:S338–S354.
2. Huliyurdurga Srinivasasetty NS, Thagachagere Ramegowda R, Kharge J, Bachahalli Krishnanayak G, S Patil S, Raj V, et al. Unusual non progressive idiopathic giant ascending aortic aneurysm-A rarity. Int J Surg Case Rep 2016;25:203–6.
3. Elefteriades JA, Rizzo JA. Epidemiology prevalence incidence trends. In: Elefteriades J, editor. Acute aortic disease. New York: Informa Healthcare; 2007. p.89–98.
4. Kälsch H, Lehmann N, Möhlenkamp S, Becker A, Moebus S, Schmermund A, et al. Body-surface adjusted aortic reference diameters for improved identification of patients with thoracic aortic aneurysms: results from the population-based Heinz Nixdorf Recall study. Int J Cardiol 2013;163:72–8.
5. Itani Y, Watanabe S, Masuda Y, Hanamura K, Asakura K, Sone S, et al. Measurement of aortic diameters and detection of asymptomatic aortic aneurysms in a mass screening program using a mobile helical computed tomography unit. Heart Vessels 2002;16:42–5.
6. Wongwanit C, Mutirangura P, Chierakul N, Chaiyasoot W, Phongraweewan O. Rapidly enlarging and asymptomatic abdominal aortic aneurysm in a male patient with chronic obstructive pulmonary disease: A case report of endovascular aortic aneurysm repair (EVAR). Siriraj Med J 2006:58;812–8.
7. Aggarwal S, Qamar A, Sharma V, Sharma A. Abdominal aortic aneurysm: A comprehensive review. Exp Clin Cardiol 2011;16:11–5.
8. Schermerhorn M. A 66-year-old man with an abdominal aortic aneurysm: review of screening and treatment. JAMA 2009:302;2015–22.
9. Harris LM, Faggioli GL, Fiedler R, Curl GR, Ricotta JJ. Ruptured abdominal aortic aneurysms: factors affecting mortality rates. J Vasc Surg 1991;14:812–8.
10. Davies RR, Gallo A, Coady MA, Tellides G, Botta DM, Burke B, et al. Novel measurement of relative aortic size predicts rupture of thoracic aortic aneurysms. Ann Thorac Surg 2006;81:169–77.
11. Johansson G, Markström U, Swedenborg J. Ruptured thoracic aortic aneurysms: a study of incidence and mortality rates. J Vasc Surg 1995;21:985–8.
12. Prapassaro T, Chinsakchai K, Techarattanaprasert S, Wongwanit C, Ruansetakit C, Hongku K, et al. Determining perioperative mortality in patients with ruptured abdominal aortic aneurysm: Insights from a retrospective cohort study. Siriraj Med J 2024:76; 480–7.
13. Asouhidou I, Asteri T. Acute aortic dissection: be aware of misdiagnosis. BMC Res Notes 2009;2:25.
14. Chung JH, Ghoshhajra BB, Rojas CA, Dave BR, Abbara S. CT angiography of the thoracic aorta. Radiol Clin North Am 2010;48:249–64.
15. McMahon MA, Squirrell CA. Multidetector CT of Aortic Dissection: A Pictorial Review. Radiographics 2010;30:445–60.
16. Kapustin AJ, Litt HI. Diagnostic imaging for aortic dissection. Semin Thorac Cardiovasc Surg 2005;17: 214–23.
17. Nienaber CA, von Kodolitsch Y, Nicolas V, Siglow V, Piepho A, Brockhoff C, et al. The diagnosis of thoracic aortic dissection by noninvasive imaging procedures. N Engl J Med 1993;328:1–9.

18. Mao SS, Ahmadi N, Shah B, Beckmann D, Chen A, Ngo L, et al. Normal thoracic aorta diameter on cardiac computed tomography in healthy asymptomatic adults: impact of age and gender. Acad Radiol 2008;15: 827–34.
19. Stein E, Mueller GC, Sundaram B. Thoracic aorta (multidetector computed tomography and magnetic resonance evaluation). Radiol Clin North Am 2014; 52:195–217.
20. Kimura-Hayama ET, Meléndez G, Mendizábal AL, Meave-González A, Zambrana GFB, Corona-Villalobos CP. Uncommon congenital and acquired aortic diseases: role of multidetector CT angiography. Radiographics 2010;30:79–98.
21. Liotta R, Chughtai A, Agarwal PP. Computed tomography angiography of thoracic aortic aneurysms. Semin Ultrasound CT MR 2012;33:235–46.
22. Prabhasavat, K. Measurement of the aortic diameter in the asymptomatic Thai population in Siriraj Hospital: Assessment with multidetector CT. Siriraj Med J 2016;68: 247–56.
23. Siriapisith T, Tongdee T, Tongdee R, Jitnuson P, Karuvanarint S. CT criteria for differentiation between true and false lumen in aortic dissection. Siriraj Med J 2004;56:410–17.
24. Kooiman J, Pasha SM, Zondag W, Sijpkens YWJ, van der Molen AJ, Huisman MV, et al. Meta-analysis: serum creatinine changes following contrast enhanced CT imaging. Eur J Radiol 2012;81:2554–61.
25. Solomon R. Contrast-medium-induced acute renal failure. Kidney Int 1998;53:230–42.
26. Morcos SK, Thomsen HS, Webb JA. Contrast-media-induced nephrotoxicity: a consensus report. Contrast Media Safety Committee, European Society of Urogenital Radiology (ESUR). Eur Radiol 1999;9: 1602–13.
27. Rudnick MR, Goldfarb S, Wexler L, Ludbrook PA, Murphy MJ, Halpern EF, et al. Nephrotoxicity of ionic and nonionic contrast media in 1196 patients: a randomized trial. The Iohexol Cooperative Study. Kidney Int 1995;47:254–61.
28. Pistolesi V, Regolisti G, Morabito S, Gandolfini I, Corrado S, Piotti G, et al. Contrast medium induced acute kidney injury: a narrative review. J Nephrol 2018;31:797–812.
29. Karlsberg RP, Dohad SY, Sheng R. Contrast-induced acute kidney injury (CI-AKI) following intra-arterial administration of iodinated contrast media. J Nephrol 2010;23:658–66.
30. Karlsberg RP, Dohad SY, Sheng R. Contrast medium-induced acute kidney injury: comparison of intravenous and intraarterial administration of iodinated contrast medium. J Vasc Interv Radiol 2011;22:1159–65.
31. Mohammed NM, Mahfouz A, Achkar K, Rafie IM, Hajar R. Contrast-induced Nephropathy. Heart Views 2013;14:106–16.
32. Choorat S, Totanarungroj K, Muangman, N. Assessment of normal subcarinal angle on chest radiographs in adult Thai population. Siriraj Med J 2008;60:264–6.
33. Somcharit L. Traumatic Hemothorax and Pneumothorax detected by EFAST Compared with Chest Radiography at Siriraj Hospital. Siriraj Med J 2016;68:171–6.
34. Hiratzka LF, Bakris GL, Beckman JA, et al. 2010. ACCF/AHA/AATS/ACR/ASA/SCA/SCAI/SIR/ STS/SVM guidelines for the diagnosis and management of patients with Thoracic Aortic Disease: a report of the American College of Cardiology Foundation/American Heart Association Task Force on Practice Guidelines, American Association for Thoracic Surgery, American College of Radiology, American Stroke Association, Society of Cardiovascular Anesthesiologists, Society for Cardiovascular Angiography and Interventions, Society of Interventional Radiology, Society of Thoracic Surgeons, and Society for Vascular Medicine. Circulation 2010;122:e410.
35. Riambau V, Böckler D, Brunkwall J, Cao P, Chiesa R, Coppi G, et al. Editor's choice - management of descending thoracic aorta diseases: clinical practice guidelines of the European Society for Vascular Surgery (ESVS). Eur J Vasc Endovasc Surg 2017;53:4–52.
36. Fultz PJ, Melville D, Ekanej A, Holzwasser G, Voci S, Wandtke JC, et al. Nontraumatic rupture of the thoracic aorta: chest radiographic features of an often unrecognized condition. AJR Am J Roentgenol 1998;171:351–7.
37. Seltzer SE, D'Orsi C, Kirshner R, DeWeese JA. Traumatic aortic rupture: plain radiographic findings. AJR Am J Roentgenol 1981;137: 1011–4.
38. Marnocha KE, Maglinte DD, Woods J, Goodman M, Peterson P. Mediastinal-width/chest-width ratio in blunt chest trauma: a reappraisal. AJR Am J Roentgenol 1984;142:275–7.
39. Pham MHC, Sigvardsen PE, Fuchs A, Kühl JT, Sillesen H, Afzal S, et al. Aortic aneurysms in a general population cohort: prevalence and risk factors in men and women. Eur Heart J Cardiovasc Imaging 2024;25:1235–43.